JOURNAL OF MATERIALS SCIENCE 27 (1992) 2792–2798

Effect of rapid solidification on mechanical properties of Cu–Al–Ni shape memory alloys

S. S. LEU, Y. C. CHEN, R. D. JEAN
Materials Research Laboratory, Industrial Technology Research Institute, Hsinchu 31015, Taiwan

Mechanical properties of β-phase shape memory alloys with the addition of small amounts of chromium or zirconium were studied at various temperatures. In addition to the conventional casting process, Cu–Al–Ni–Zr alloys were produced by rapidly solidified processes, including the gas atomization and melt spinning methods. Buck materials were also made by hot-press sintering from the Cu–Al–Ni–Zr alloy powders and chopped ribbons. It was found that the brittleness of Cu–Al–Ni alloys was improved by the addition of either chromium or zirconium. It is suggested that this improvement is due to increase of grain-boundary strength, not just because of grain refining. The better mechanical properties were obtained in the rapidly solidified and sintered alloys which show fine grain size, fracture strength as high as 780 MPa and 7% fracture strain.

1. Introduction

The shape memory alloys (SMA) which exhibit shape memory effect and pseudoelasticity due to the thermoelastic character of martensitic transformation are well known [1, 2]. Among the various shape memory alloys, the copper-based SMA are particularly attractive because of their low cost and easy processing. Unfortunately, the polycrystalline copper-based SMA usually exhibit limited ductility, especially for Cu–Al–Ni alloys [3–5]. The brittleness of these alloys caused by intergranular fracture has been attributed to a high elastic anisotropy and large intrinsic grain size in Cu–Al–Ni alloys [3]. Recently many efforts have been made to reduce the grain size of Cu–Al–Ni alloys, either by adding grain-refining elements such as zirconium, titanium etc. [5–8], or by rapid solidification processes [9–12]. Successful results of grain refinement have been obtained using the above methods. Cu–Al–Ni alloys with the addition of zirconium or titanium show transgranular fracture and improved ductility. However, a Cu–Al–Ni alloy ribbon made by melt spinning having a fine grain size of about 1 μm is still brittle and exhibits intergranular fracture [10]. This indicates that the large grain size is not the only embrittlement factor in Cu–Al–Ni alloys. Currently, some experimental results have ascribed the intergranular fracture found in Cu–Al–Ni alloys to the segregation of oxygen at grain boundaries [8, 10].

The yield stress, fracture stress, elongation and strain–stress curve of a Cu–Al–Ni alloy are strongly dependent on the test temperature and its martensitic transformation temperature [3, 5]. Consequently, they are dependent on the alloy composition because the martensitic transformation temperature of Cu–Al–Ni alloys is a function of the alloy composition. However, only a few experimental results have taken the effects of temperature into account when the improvement of ductility of Cu–Al–Ni alloys by grain refinement was evaluated.

In the present study, the mechanical properties of Cu–Al–Ni alloys modified with additions of chromium or zirconium, and/or solidified by gas atomization and melt-spinning processes are investigated. Bulk specimens were made by hot-press sintering from Cu–Al–Ni powders and melt-spun ribbons, then followed by hot rolling. Tensile tests were carried out at various temperatures compared with the phase-transformation temperatures for each alloy.

2. Experimental procedure

The original Cu–Al–Ni alloy designed to contain 14 wt % Al and 4 wt % Ni was prepared from 99.99% pure copper, 99.9% pure aluminium and 99.5% pure nickel. The alloy was melted in an induction furnace under an argon atmosphere and cast in a ceramic shell mould. This primary Cu–Al–Ni alloy is denoted C1, where C indicates the cast sample. Some of primary Cu–Al–Ni alloy ingots were remelted and alloyed with 0.5 wt % zirconium or chromium for grain refinement. The cast alloys containing chromium or zirconium are denoted C2 and C3, respectively.

In order to reduce the grain size further, Cu–Al–Ni–Zr alloy powders and ribbons made from Alloy C3 were produced by gas atomization and single-roller melt spinning processes, respectively. Both powders and chopped ribbons were sintered by hot pressing at 900 °C under a pressure of 10 MPa. The sintered Cu–Al–Ni–Zr alloys made from powders and melt-spun ribbons are denoted S1 and S2, respectively. The analysed compositions of the five alloys are listed in Table 1, where the nominal composition of

0022–2461

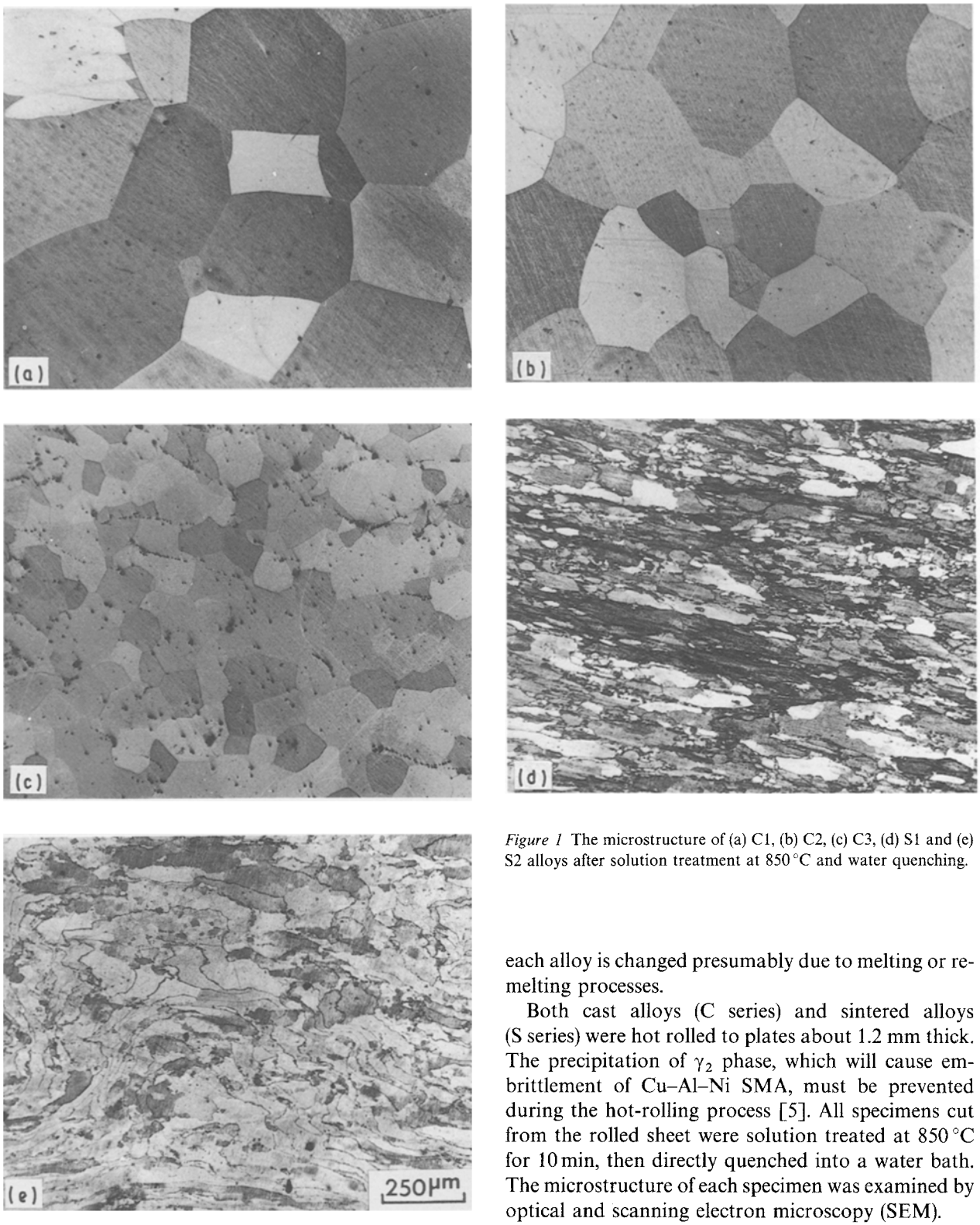

Figure 1 The microstructure of (a) C1, (b) C2, (c) C3, (d) S1 and (e) S2 alloys after solution treatment at 850 °C and water quenching.

TABLE I Chemical compositions (wt %) of alloys; "C" and "S" denote the cast and sintered alloys, respectively

	Alloy				
	C1	C2	C3	S1	S2
Al	13.8	13.8	13.9	14.0	13.7
Ni	3.8	4.0	4.1	4.0	4.0
Cr	–	0.2	–	–	–
Zr	–	–	0.4	0.5	0.4
Cu	bal.	bal.	bal.	bal.	bal.

each alloy is changed presumably due to melting or remelting processes.

Both cast alloys (C series) and sintered alloys (S series) were hot rolled to plates about 1.2 mm thick. The precipitation of γ_2 phase, which will cause embrittlement of Cu–Al–Ni SMA, must be prevented during the hot-rolling process [5]. All specimens cut from the rolled sheet were solution treated at 850 °C for 10 min, then directly quenched into a water bath. The microstructure of each specimen was examined by optical and scanning electron microscopy (SEM).

A resistance measurement technique was employed to obtain the martensitic transformation temperature (MTT) for each alloy after solution treatment. The transformation temperatures M_s and M_f (the starting and finishing temperatures for transformation of austenite to martensite) and A_s and A_f (the starting and finishing temperatures for reverse transformation of martensite to austenite) were obtained from the change of electric resistance during cooling and heating cycles. In addition, the oxygen content of each alloy was measured using a nitrogen/oxygen determinator of LECO TC-136.

Tensile tests of plate-type specimens were conducted at various temperatures with a strain rate of

0.01 min^{-1}. The tensile strain was measured with an MTS extensometer. To study the shape memory capability, some specimens were loaded up to 2% strain, then gradually unloaded under the same strain rate. On the other hand, yielding stress, fracture stress and elongation were measured from tensile curves of other specimens. The fracture surfaces of specimens after tensile tests were examined by SEM.

3. Results and discussion

3.1. Microstructure

All the alloys after solution treatment and water quenching exhibit fully parent phase, as shown in Fig. 1. The C1 alloy (primary alloy) exhibits a large intrinsic grain size of about 460 μm which is determined by the linear intercept method. Several inclusions are noted in the matrix. The C2 alloy which contains 0.2 wt % Cr shows coarse grain structure, as in the C1 alloy. For the C3 alloy, addition of 0.4 wt % Zr reduces markedly the grain size down to about 80 μm. Many more inclusions or second-phase particles are present in this alloy.

The grain sizes of alloys S1 and S2 shown in Fig. 1d and e are much smaller than those of cast alloys. They seem to be equivalent to the diameter of powders and the thickness of chopped ribbon prior to hot pressing, respectively. Distinct boundaries corresponding to the free surface of each powder or chopped ribbon are visible in both S1 and S2 alloys.

3.2. Tensile testing at room temperature

The mechanical properties of alloys were determined by tensile testing at room temperature. Typical tensile curves of five alloys are shown in Fig. 2. The corresponding yield stress, σ_y, tensile strength, σ_f, and elongation, i.e. fracture strain, ε_f, are also listed in Fig. 2. It can be seen that the elongation and fracture strength of the C1 alloy are only 0.8% and 260 MPa, respectively. For the C2 alloy, the elongation is about 3.8%, and the tensile strength is 666 MPa. This indicates that the brittleness of Cu–Al–Ni SMA is improved remarkably due to the addition of 0.2 wt % Cr. A similar improvement of mechanical properties is also obtained in the C3 alloy by the addition of

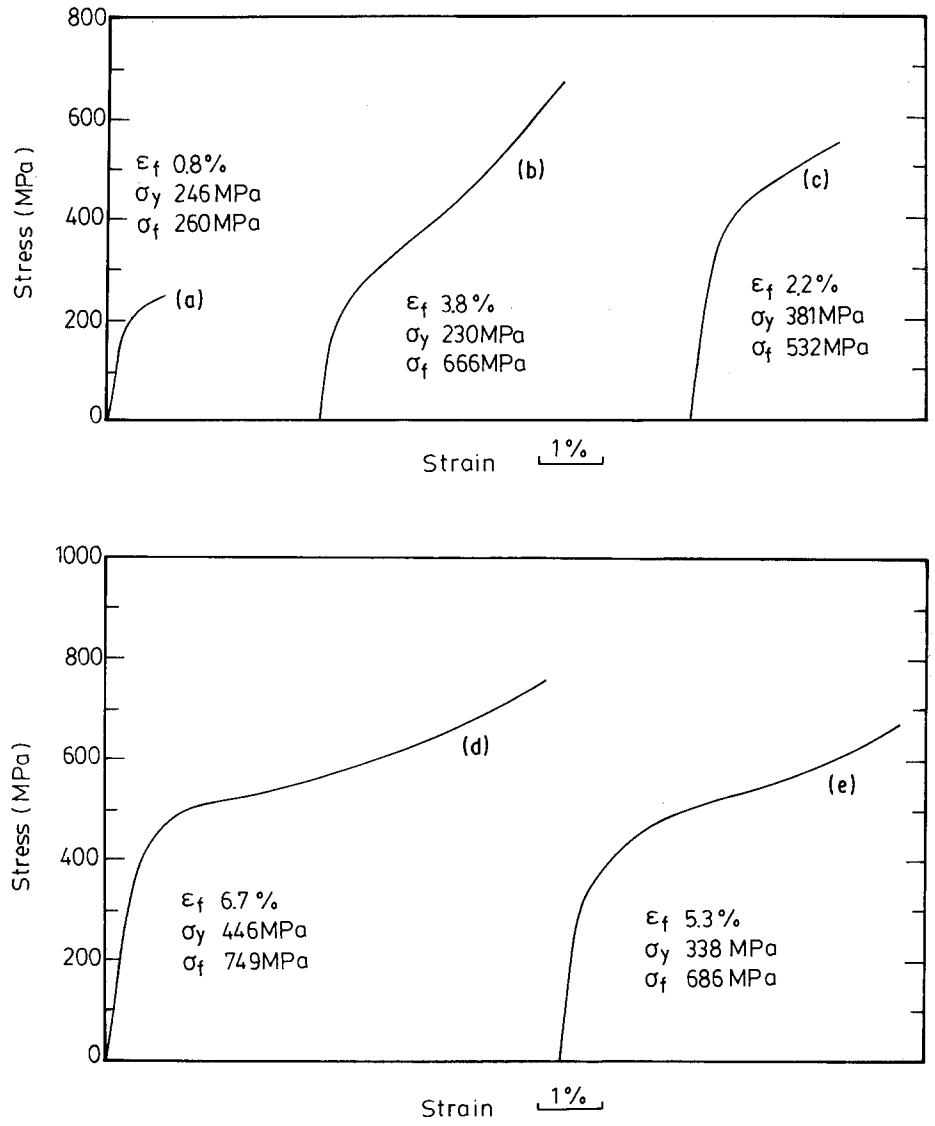

Figure 2 Typical stress–strain tensile curves of specimens tested at room temperature. The corresponding elongation, ε_f, yield stress, σ_y, and tensile stress, σ_f, are also listed,

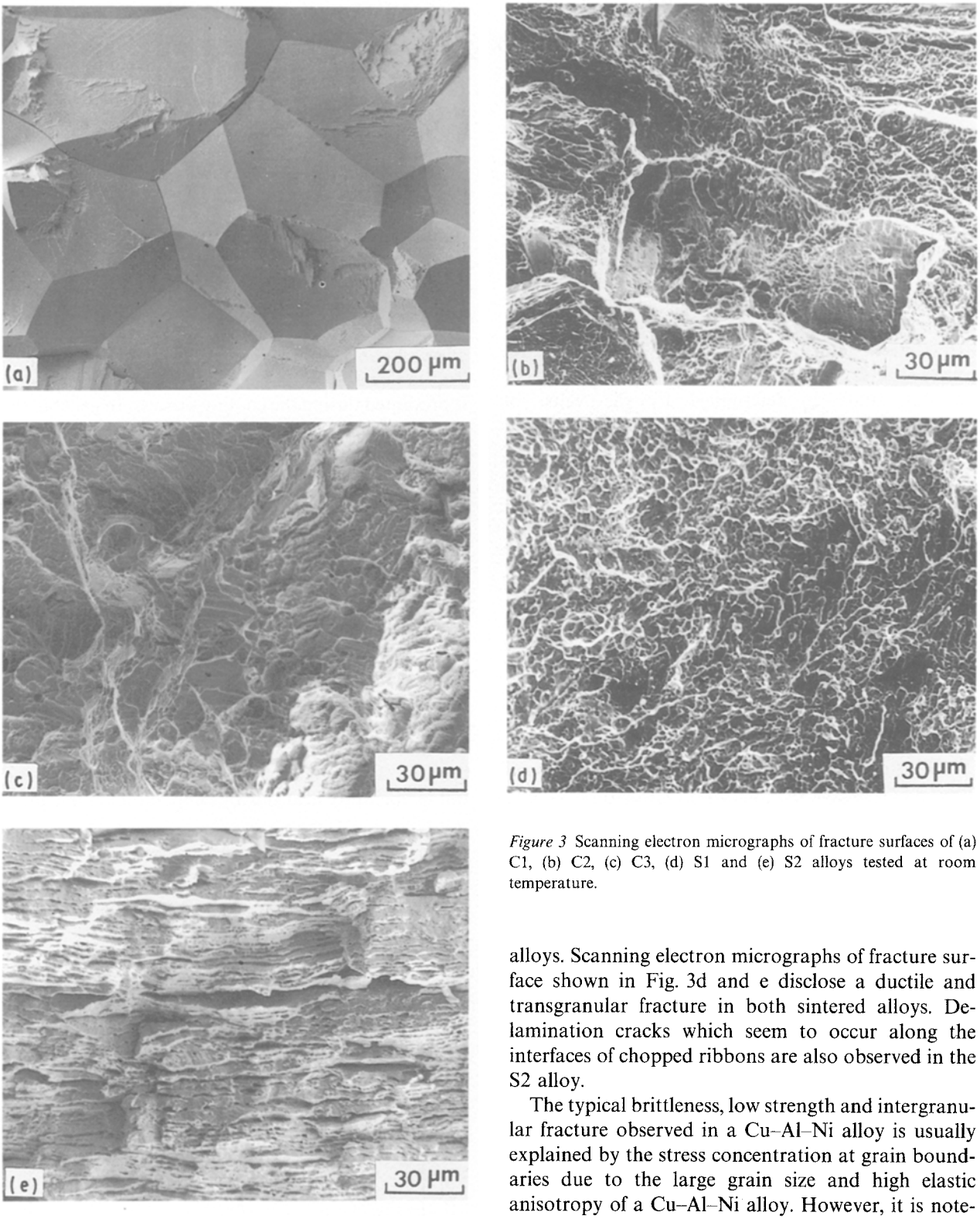

Figure 3 Scanning electron micrographs of fracture surfaces of (a) C1, (b) C2, (c) C3, (d) S1 and (e) S2 alloys tested at room temperature.

zirconium. Fracture surfaces of tensile specimens examined by SEM are shown in Fig. 3. The intergranular fracture, which is an intrinsic characteristic of a Cu–Al–Ni alloy, is observed in the C1 alloy. However, addition of either chromium or zirconium to C1 alloy changes the fracture mode from intergranular to transgranular as shown in Fig. 3b and c.

On the other hand, much better tensile properties are obtained in both sintered alloys, as shown in Fig. 2d and e. The elongations are as high as 6.7% and 5.3% for S1 and S2 alloys, respectively. The tensile strengths are also greater than those for the cast alloys. Scanning electron micrographs of fracture surface shown in Fig. 3d and e disclose a ductile and transgranular fracture in both sintered alloys. Delamination cracks which seem to occur along the interfaces of chopped ribbons are also observed in the S2 alloy.

The typical brittleness, low strength and intergranular fracture observed in a Cu–Al–Ni alloy is usually explained by the stress concentration at grain boundaries due to the large grain size and high elastic anisotropy of a Cu–Al–Ni alloy. However, it is noteable that the grain size of the C2 alloy is close to that of the C1 alloy, but the tensile strength and elongation of the C2 alloy is improved greatly. In addition, the fracture mode is also changed from intergranular in the C1 alloy to transgranular in the C2 alloy. Consequently, the grain-boundary strength in the C2 alloy is obviously improved due to addition of chromium, if other material properties, such as the elastic anisotropy and the matrix strength, are assumed to be similar in both C1 and C2 alloys. This indicates that large grain size is not an exclusive factor contributing to the embrittlement of Cu–Al–Ni SMA. In the present study, it was found that oxygen concentration decreased remarkably in the cast alloys containing

either chromium or zirconium. This suggests that either chromium or zirconium is a scavenger for oxygen and may avoid segregation of oxygen at grain boundaries, as proposed by Lee and Wayman [8]. Therefore, grain-boundary strength might be improved due to the addition of chromium or zirconium. This results in transgranular fracture instead of intergranular fracture.

The shape recovery, i.e. pseudoelasticity of the alloys, was investigated by straining the specimens up to 2% and releasing the load immediately. Except for the C1 alloy which fractured before the strain reached 2%, the loading and unloading curves for the other four alloys are illustrated in Fig. 4. Although each stress–strain loop is different, they all exhibit good shape recovery capability. The ratio of shape recovery in this study is determined by the value of $(\varepsilon_{max} - \varepsilon_p)/\varepsilon_{max}$, where ε_{max} is the maximum strain during testing (2% in this study), ε_p is the residual plastic strain after unloading. The results indicate that the recovery ratios of all alloys are larger than 97%.

The M_s temperatures of five alloys measured through the variation of electric resistance are shown in Fig. 5. The martensitic transformation temperatures (MTT) of all the alloys are lower than room temperature. This confirms the previous result that the parent phase is the existing phase at room temperature for all the alloys. Therefore, the pseudoelastic behaviour of the parent phase was observed in each alloy, as shown in Fig. 4. The MTT are evidently different in each alloy, as shown in Fig. 5. Many factors will affect the MTT of copper-based SMA, including the external force [12], degree of ordering [13], thermal cycling [14], grain size of β grains [15] and chemical compositions of alloys [16, 17]. However, in the present study, only grain size and composition factors are concerned. In Cu–Zn–Al SMA, Adnyana reported that the M_s temperature rose by about 15 °C due to a full growth of β grains [15]. However, the MTT would shift more than a hundred degrees by modification of compositions. Therefore, it is thought that the remarked difference in MTT between those alloys is due to the differences in chemical compositions, as given in Table I.

The martensitic transformation of alloy ribbon before hot pressing was also investigated and is shown in Fig. 5f. It is interesting that the M_f temperature of the alloy ribbon is much lower than that of the others. This indicates that further growth of martensite plates is prevented during the cooling process. In general, the rapid solidification materials contain extraordinarily fine grains [10]. It is believed that the decrease of M_f temperature observed in melt-spun ribbon is due to the constraint of fine grains.

3.3. Tensile testing at various temperatures

It is well known that the stress–strain behaviour of a Cu–Al–Ni SMA is a function of test temperature [3]. In pseudoelastic alloys, the yielding stress, σ_y, is the stress required for nucleation of stress-induced martensite. Fig. 6 shows the results of the tensile test of the C2 alloy under various test temperatures. The values of σ_y decrease continuously as the test temperatures decrease. The minimum yielding stress is obtained at a test temperature near the M_s temperature of the alloy,

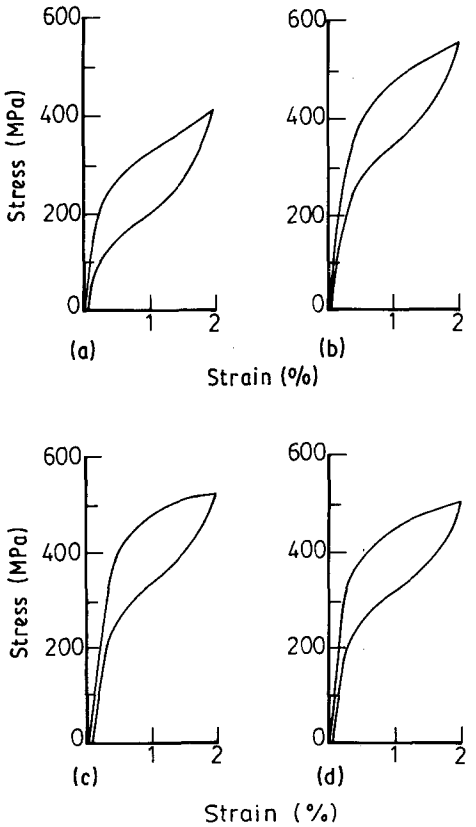

Figure 4 The capability of shape recovery is displayed by the tensile curves of specimens (a) C2, (b) C3, (c) S1, (d) S2 during loading and unloading processes.

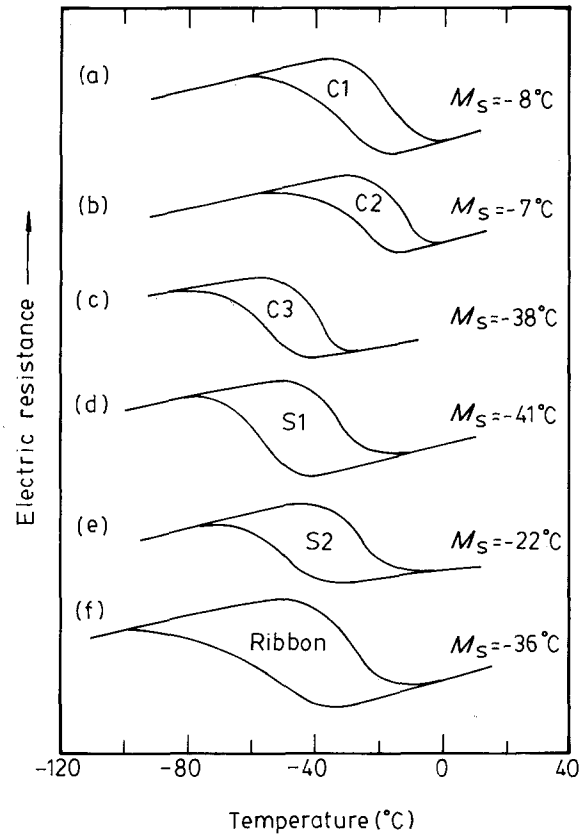

Figure 5 The variations of electric resistance in (a) C1, (b) C2, (c) C3, (d) S1, (e) S2 and (f) alloy ribbon during martensitic transformation.

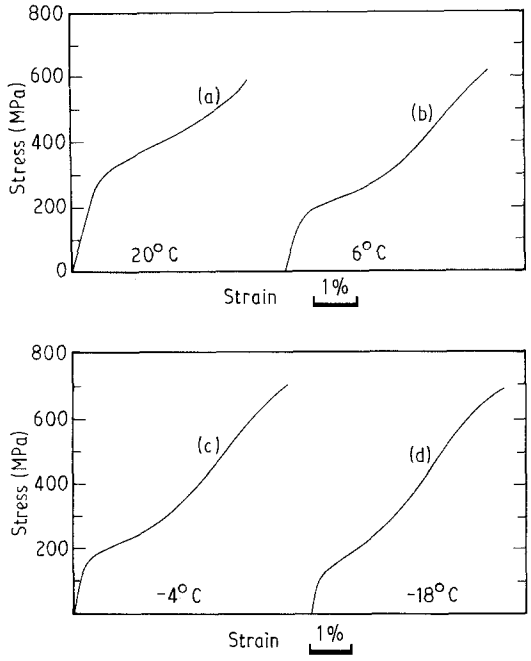

Figure 6 The stress–strain tensile curves of C2 alloy tested at various temperatures.

as shown in Fig. 6d. However, a slightly higher tensile strength, σ_f, and larger elongation, ε_f, were obtained at a test temperature close to the M_s temperature.

As mentioned previously, the tensile properties were improved on decreasing the test temperature. For comparison, each alloy was tested at a specific lower temperature which was chosen to be close to its M_s temperature. Basically, the difference between the testing temperature and the M_s temperature is less than 5 °C. The results are shown in Fig. 7. The elongation and tensile strength for the C1 alloy are 2.9% and 350 MPa, respectively. For the C2 and C3 alloys, the tensile properties were improved through additions of either elemental chromium or zirconium, especially in the tensile strength. On the other hand, the best tensile properties were observed in both sintered alloys. The elongation of S1 alloy is as high as 7.0%, as shown in Fig. 7d. Furthermore, SEM examinations revealed that the fracture modes of specimens tested at lower temperatures are similar to those tested at room temperature, i.e. intergranular fracture was shown in the C1 alloy and transgranular fracture was observed in the other alloys.

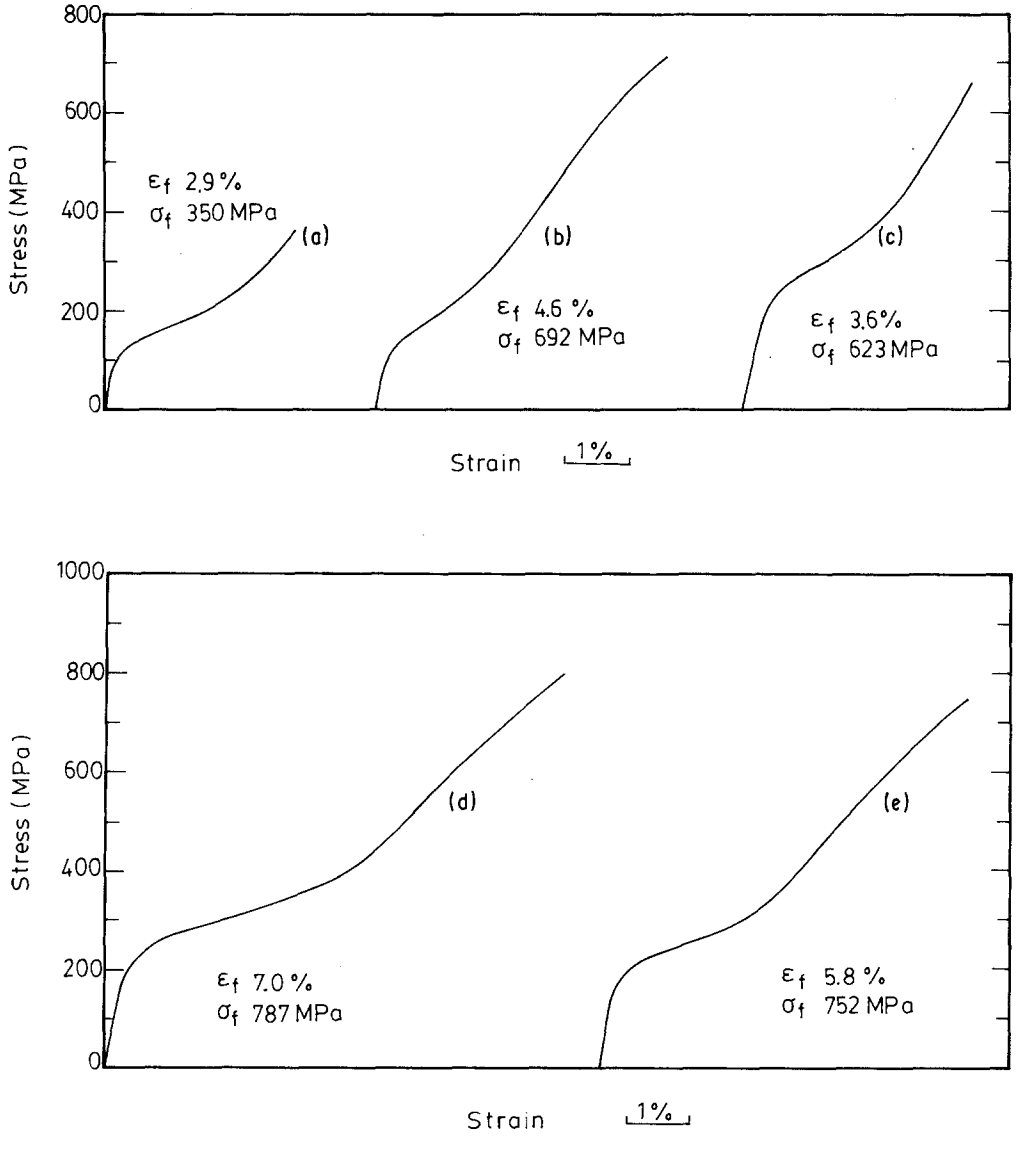

Figure 7 The typical tensile curves of alloys (a) C1, (b) C2, (c) C3, (d) S1, (e) S2 tested at a temperature near the M_s temperature of the alloys.

It has been reported that the elongation of a Cu–Al–Ni SMA having large grains is only about 1% [9]. For the C1 alloy tested close to its M_s temperature, the elongation rose markedly from 0.8% to 2.9% although the tensile strength increased slightly . The other four alloys showed similar improved ductility. This indicates that the ductility of a Cu–Al–Ni alloy is dependent on the test temperature. Therefore, it is suggested that the ductility of Cu–Al–Ni alloys should be evaluated at several temperatures instead of at room temperature only. The present study finds that the addition of chromium or zirconium indeed improves ductility of Cu–Al–Ni alloys. Hot-press sintering of Cu–Al–Ni–Zr powders or chopped ribbons yields even better mechanical properties.

4. Conclusion

Effects of grain-refining elements and rapid solidification on the mechanical properties of Cu–Al–Ni SMA have been investigated. The results are summarized as follows:

1. The addition of a small amount of chromium to the ternary Cu–Al–Ni SMA gives improved ductility and increased fracture strength. The fracture mode was also changed from intergranular to transgranular by this alloying effect. However, the grain size remains the same as that in the ternary Cu–Al–Ni SMA. This indicates that the grain-boundary properties of Cu–Al–Ni SMA were improved due to addition of chromium.

2. Much smaller grains were obtained in the sintered Cu–Al–Ni–Zr alloys made from powders or chopped ribbons. Better mechanical properties were shown in these alloys. Their tensile strength and elongation were as high as 780 MPa and 7.0%, respectively.

3. On decreasing the tensile test temperature to about M_s, the elongations of Cu–Al–Ni alloys increase; however, the tensile strength and fracture mode are almost unchanged.

4. The mechanical properties of SMA are a function of testing temperature. Comparison of the mechanical properties of SMA is suggested to be carried out at the same temperature difference between testing temperatures and M_s temperatures.

References

1. H. WARLIMONT, L. DELAEY, R. V. KRISHNAN and H. TAS, *J. Mater. Sci.* **9** (1974) 1521.
2. A. NAGASAWA, K. ENAMI, Y. ISHINO, Y. ABE and S. NENNO, *Scripta Metall.* **8** (1974) 1055.
3. K. OTSUKA, C. M. WAYMAN, K. NAKAI, H. SAKAMOTO and K. SHIMIZU, *Acta Metall.* **24** (1976) 207.
4. H. SAKAMOTO, K. SHIMIZU and K. OTSUKA, *Trans. Jpn Inst. Metals* **26** (1985) 638.
5. G. N. SURE and L. C. BROWN, *Metall. Trans.* **15A** (1984) 1613.
6. J. S. LEE and C. M. WAYMAN, *Metallography* **19** (1986) 401.
7. R. ELST, J. van HUMBEECK and L. DELAEY, *Mater. Sci. Technol.* **4** (1988) 644.
8. J. S. LEE and C. M. WAYMAN, *Trans. Jpn Inst. Metals* **27** (1986) 584.
9. S. EUCKEN, P. DONNER and E. HORNBOGEN, *Mater. Sci. Engng* **98** (1988) 469.
10. S. MATSUOKA, M. HASEBE, R. OSHIMA and F. E. FUJITA, *Jpn J. Appl. Phys.* **22** (1983) 528.
11. S. W. HUSAIN, M. AHMED and P. C. CLAPP, *J. Mater. Sci.* **23** (1988) 1030.
12. H. WARLIMONT, L. DELAEY, R. V. KRISHNAN and H. TAS, *ibid.* **9** (1974) 1545.
13. A. PLANES, J. L. MACQUERON, M. MORIN and G. GUENIN, *Mater. Sci. Engng* **50** (1981) 53.
14. Y. NAKATA, T. TADAKI and K. SHIMIZU, *Trans. Jpn Inst. Metals* **26** (1985) 646.
15. D. N. ADNYANA, *Metallography* **18** (1985) 187.
16. N. F. KENNON, D. P. DUNNE and L. MIDDLETON, *Metall. Trans.* **13A** (1982) 551.
17. N. MWAMBA and L. DELAEY, *J. Phys. (Paris) Colloq. C4* **43** (1982) 715.

Received 29 January
and accepted 7 June 1991